MONITORING THE ABRASIVE BLASTING PROCESS USING STRAIN GAUGE FORCE MEASUREMENT

JIRI NEUWIRTH[2], DAVID ZUROVEC[1], JAKUB HLOSTA[1], JAN DIVIS[1], JIRI ROZBROJ[1], LEO KASPERCIK[1], FRANTISEK KOPECKY[1], JIRI DOBIAS[1], JAN NECAS[1]

[1]VSB-Technical University of Ostrava, Faculty of Mining and Geology, Department of Mining Engineering and Safety, 17. listopadu 15/2172, 708 00, Ostrava-Poruba, Czech Republic

[2]WISTA s.r.o., Dlouhe dily 414, 763 02, Zlin-Louky, Czech Republic

DOI: 10.17973/MMSJ.2026_11_2026098

e-mail: david.zurovec@vsb.cz

ABSTRACT

The abrasive blasting process is designed for blasting structurally complex components or structures. The target of blasting is to achieve an optimal surface finish on structures, for example, prior to the application of an anti-corrosion coating. The effectiveness of abrasive blasting technology is highly sensitive to the settings of key operating conditions, which include air pressure and air flow rate, the amount and type of abrasive material, and the size of the nozzle. The aim of this research is to determine the influence of the settings of selected key operating parameters on the forces acting on the nozzle holder and the blasting plate platform. Brown fused alumina abrasive material in various particle size distribution was used for the experimental verification. The results demonstrated the applicability of this method for automating the adjustment of operating conditions in the blasting process to ensure continuous operation.

KEYWORDS

Blasting process, abrasive material, brown fused alumina.

1 INTRODUCTION

This research project focuses on monitoring the efficiency of the blasting process and optimizing the operating parameters of a semi-automated system, both in terms of the design of structural components and the integration of sensor and control systems, with the aim of ensuring intelligent control and monitoring of the blasting process [Glienke 2025, Hansel 2000, Mellali 1997, Nguyen 2024, Pratap 2025]. The experimental blasting unit consists of a compact blasting chamber equipped with a five-axis manipulator, which enables automated blasting of serial steel structures in a closed environment. This solution reflects current industrial production requirements, which emphasize repeatability, surface finish quality, and minimizing the need for human intervention. The use of a robotic manipulator significantly increases productivity and reduces the variability of results caused by the human factor, leading to the consistent achievement of target surface treatment parameters. The design of the blasting chamber is based on the principle of a pressurized closed system, which ensures both the effective separation of abrasive and dust from the external environment and control over internal conditions during operation. The system consists of several main functional subsystems: a compressor unit, an air treatment system (including a dryer and separators), a filtration unit (HEPA filter, cartridge filters, fan, air tank, and waste container), as well as the blasting system itself, consisting of a cyclone separator, screen, abrasive hopper, and pressure vessel or injector, and a blasting chamber with a manipulator [Int-enviroguard 2024]. As part of the project development, the booth was further expanded to include comprehensive sensor equipment enabling detailed monitoring and recording of all key operating parameters [Begg 2016, Bobzin 2016, Int.EnviroGuard 2024, Varacalle 2006]. The monitoring system includes sensors measuring air pressure and flow, humidity in the work area, temperature, abrasive level, and abrasive mass flow, as well as strain gauge sensors for monitoring the condition of the equipment during operation. The measurement setup of the abrasive blasting system is shown in Fig. 1.

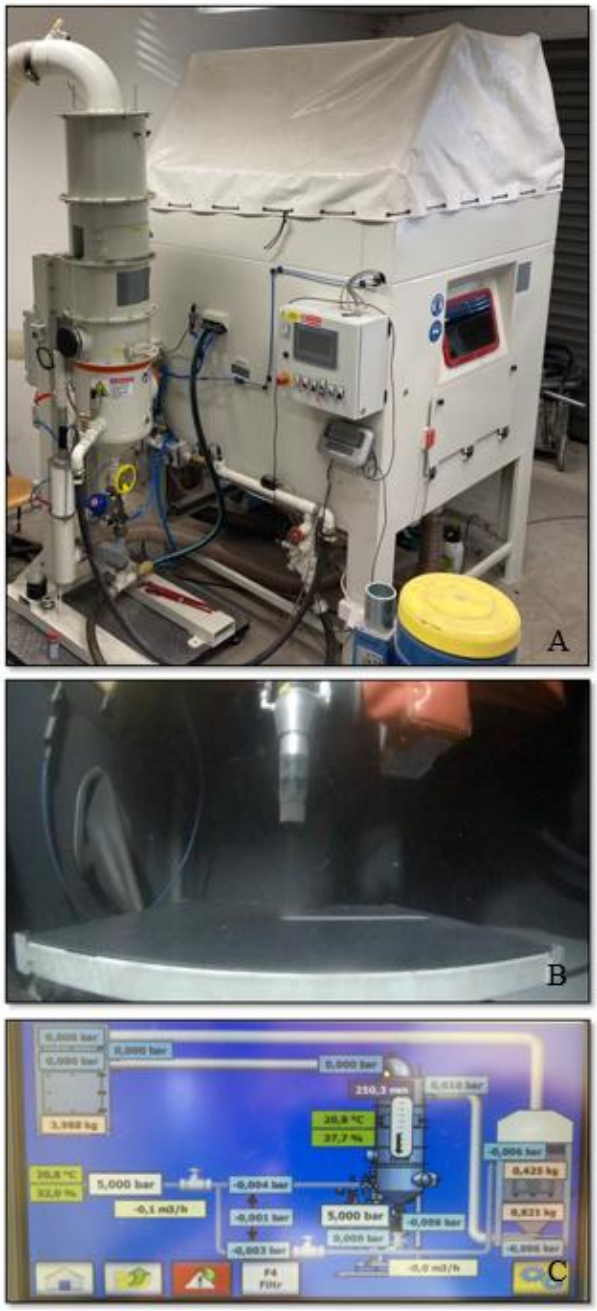


Figure 1. Measuring assembly for an abrasive blasting system: A) Blasting system assembly, B) Blasting process inside the blasting chamber, C) Control panel

2 MATERIALS AND METHODS

Brown fused alumina, available in four grain size fractions, was used for experimental studies of the efficiency of abrasive blasting. Brown fused alumina consists almost entirely of aluminum oxide and is nearly iron-free. Brown fused alumina is less pure than white fused alumina. The unique composition of this angular mineral makes it extremely stable. It is also both hard and tough. Brown fused alumina is primarily used as a blasting medium. [CERABLAST 2026]. The individual grain size fractions of brown fused alumina are shown in SEM photographs; see Figure 2. From this detailed image, the shape of the individual particles, which have a sharp-edged character, can be characterized. Furthermore, an analysis of the basic properties of the individual fractions of brown fused alumina was conducted [Zegzulka 2020, Kruszelnicka 2021], which are listed in Tab. 1. A comparison of the measured properties reveals differences in the granulometric distribution between the individual samples of brown fused alumina. Significant differences are observed in the flow function, where the fine-grained brown fused alumina sample F220 exhibits very good flow properties compared to the coarse-grained sample F24, which falls on the boundary between free-flowing and poorly flowing materials. There are no significant differences between the individual samples when comparing the effective angle of internal friction. In terms of bulk density, the values between the individual samples differ by no more than 5%. The particles are angular and are shown in the SEM images in Fig. 2

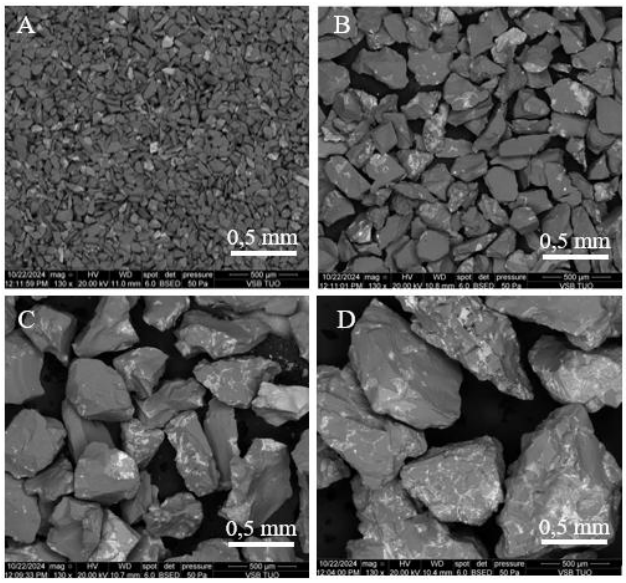


Figure 2. Microscopic images of individual particle size fractions of brown fused alumina: A) F220, B) F80, C) F46, D) F24

			F220	F80	F46	F24
Particle size distribution	d_{10}	[µm]	47,7	158	317	658
	d_{50}	[µm]	77,9	236	457	944
	d_{90}	[µm]	124	348	659	1430
Angle of internal friction	ϕ_{ef}	[°]	36,5	34,9	34,4	37,6
Flow Function	ff_c	[-]	40	21	11	5
Bulk density	ρ_s	[kg/m³]	1797	1787	1825	1867

Table 1. Properties of the fractions of brown fused alumina

In this case, the effectiveness of abrasive blasting is assessed based on strain gauge measurements taken on the nozzle holder and the blasting plate platform. Zemic L6D/30kg C3 strain gauges were used for both measurement locations. The sampling frequency for the recorded data was 2 Hz. The strain gauges were calibrated to a zero value before each measurement series. Figure 3 shows the positions for force measurement, where position I denotes the strain gauge on the nozzle holder and position II denotes the strain gauge on the blasting plate platform. Semi-automated abrasive blasting technology allows for manual adjustment of the main operating conditions, which are the parameters of the inlet blasting air (air pressure and air flow rate) and the mass flow rate of the abrasive. Compressed air is generated by an ALUP air control screw compressor (ALUP). An inlet pressure in the range of 3–7.5 bar was selected for the experimental measurements. A Thomson TV II metering valve 1 1/4" MNPT (SCHMIDT) was used to regulate the abrasive material feed. The mass flow rate of the abrasive was controlled by opening a slide valve in the range of 0–100%. Compressed air carries the abrasive material into the blasting chamber via a flexible hose, which is equipped at the end with a nozzle of a defined outlet diameter. In this case, a KENNAMETAL SN159 nozzle with an inner diameter of 8 mm was used (KENNAMETAL). The distance between the nozzle and the blasted surface was set uniformly at 400 mm for all experiments. The blasted surface in this case was a 3 mm thick steel sheet with dimensions of 400x400mm. The nozzle movement speed during the blasting process was set at 30 mm/s, and the length of the blasted surface under evaluation was 300 mm. Each measurement series for the blasting process includes the time-dependent load profile. From the total measured load profile for each series, only a 10 second time interval is evaluated. Within this interval, the operating conditions of the blasting process are highly stable.

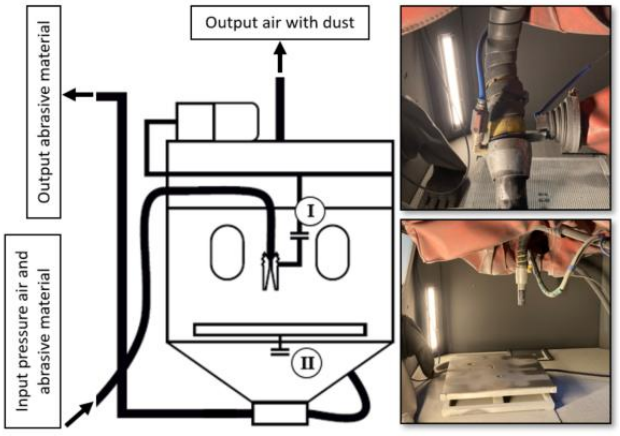


Figure 3. View of measurement points for force measurement: I—Strain gauge sensor load on the nozzle holder, II—Strain gauge sensor load on the platform of the blasting plate

3 RESULTS AND DISCUSSION

Fig. 4 to Fig. 7 show the results of experimental load measurements taken at position I—strain gauge sensor on the nozzle holder, while Fig. 8, to Fig. 11 show the results of load measurements taken at position II—strain gauge sensor on the platform of the blasting plate. The load values on the vertical axis presented in Fig. 4 to Fig. 11 are the arithmetic mean of 20 recorded values for each measurement series. The standard deviations of the measured values are provided in Table 1 and Table 2. From the measured curves, it is evident that one of the dominant parameters influencing the magnitude of the load is the pressure of the incoming blasting air. As the pressure increases, there is a significant increase in the acting forces,

which are transmitted to both the nozzle holder and the platform of the blasting plate. This phenomenon is primarily related to the increasing dynamics of the air pressure flow and the higher kinetic energy of the abrasive particles exiting the nozzle. At the same time, experimental measurements demonstrated that monitoring the force effects using strain gauge sensor I located on the nozzle holder and sensor II located on the platform of the blasting plate represents a sufficiently effective method for online monitoring of the optimal operating setting of the outlet air pressure. The measured data indicate that changes in the particle size of the abrasive did not significantly affect the response of the strain gauge sensors within the observed range. Greater differences between the tested fractions were observed in the load measurement on the nozzle holder at higher air pressures. For example, at an air pressure of 7,5 bar, the force did not exceed 35 N for the F24 abrasive (coarse-grained sample), whereas the load under the same conditions approached 40 N for the F220 abrasive (fine-grained sample). Similarly, changes in the mass flow rate of the abrasive did not result in significant changes in the load measured on the nozzle holder. These results suggest that the dominant factors influencing the magnitude of the load are primarily the system's pressure settings and the dynamics of the flowing medium, while changes in the abrasive feed rate or particle size distribution are of only secondary importance within the given experimental range. The results show a relatively linear increase in load of approximately 5 N for an increase in air pressure of 1 bar. A significant benefit of the measurements conducted, however, is the ability to conduct a detailed assessment of the forces acting on the operator during manual blasting. Strain gauge sensor I, mounted on the nozzle holder, provides valuable information on the magnitude of the reaction forces that the operator must continuously transmit and stabilize throughout the entire blasting cycle. The measured values showed that, within the monitored range of operating parameters, the resulting force reached nearly 40 N. This load represents a significant physical strain on the operator, especially during prolonged or repetitive work. From an ergonomic and safety perspective, it is therefore necessary to take these factors into account when designing the work environment, technological equipment, and in the actual job assignments of workers. Long-term exposure to high forces can lead to increased operator fatigue, excessive strain on the musculoskeletal system, and the development of health complications related primarily to unilateral muscle strain and vibrations transmitted to the upper limbs. The measurement results can thus serve not only to optimize the technological parameters of the blasting process, but also as a basis for designing ergonomic measures, automating selected work operations, or implementing robotic blasting systems, which can significantly reduce the physical strain on workers while increasing the stability and repeatability of the blasting process. The load on the platform of the blasting plate yields unstable results, with a significantly higher standard deviation than the load on the nozzle holder. Table 2 and Table 3 summarize the measured force values, using a color spectrum to indicate the statistical significance of individual measurements, and include the standard deviation.

Air pressure [bar]	Mass flow [%]	Type of brown fused alumina			
		F24	F46	F80	F220
		Load on the nozzle holder [N]			
3	0	8,8 ± 1,3	8,8 ± 1,7	8,8 ± 1,7	9,8 ± 1,1
	30	7,8 ± 1,2	6,9 ± 1,6	7,8 ± 1,4	10,8 ± 0,5
	40	6,9 ± 2,2	3,9 ± 0,7	6,9 ± 0,6	11,8 ± 1,6
	50	9,8 ± 2,9	7,8 ± 1,4	5,9 ± 0,9	9,8 ± 0,8
	60	5,9 ± 2,1	2,9 ± 0,6	4,9 ± 0,8	10,8 ± 0,8
	70	6,9 ± 3,2	6,9 ± 1,0	4,9 ± 1,4	10,8 ± 1,9
	100	12,8 ± 2,8	5,9 ± 0,9	6,9 ± 0,8	7,8 ± 1,1
4	0	12,8 ± 1,9	13,7 ± 1,8	13,7 ± 1,7	15,7 ± 0,7
	30	9,8 ± 1,8	8,8 ± 0,5	14,7 ± 1,4	15,7 ± 0,8
	40	11,8 ± 2,6	9,8 ± 1,9	13,7 ± 1,4	14,7 ± 0,6
	50	11,8 ± 2,9	11,8 ± 1,6	9,8 ± 0,6	15,7 ± 1,0
	60	11,8 ± 2,9	8,8 ± 0,7	10,8 ± 0,6	15,7 ± 0,7
	70	12,8 ± 2,0	11,8 ± 1,2	9,8 ± 0,7	14,7 ± 1,0
	100	13,7 ± 2,5	14,7 ± 1,2	9,8 ± 0,5	15,7 ± 1,0
5	0	18,6 ± 2,3	19,6 ± 0,8	16,7 ± 1,3	24,5 ± 1,7
	30	16,7 ± 2,1	14,7 ± 0,6	19,6 ± 1,0	25,5 ± 1,8
	40	16,7 ± 2,1	13,7 ± 0,8	20,6 ± 2,1	23,5 ± 0,7
	50	17,7 ± 3,0	18,6 ± 1,1	17,7 ± 0,5	23,5 ± 0,7
	60	17,7 ± 3,0	18,6 ± 1,7	15,7 ± 2,0	24,5 ± 0,6
	70	18,6 ± 2,4	13,7 ± 0,5	14,7 ± 0,6	25,5 ± 0,9
	100	18,6 ± 2,6	19,6 ± 1,5	17,7 ± 0,9	24,5 ± 0,7
5,5	0	21,6 ± 2,5	21,6 ± 0,9	24,5 ± 1,5	27,5 ± 0,5
	30	20,6 ± 2,8	16,7 ± 0,5	21,6 ± 0,5	26,5 ± 0,7
	40	25,3 ± 2,3	16,7 ± 0,5	24,5 ± 1,3	26,5 ± 0,5
	50	21,6 ± 1,6	20,6 ± 1,3	21,6 ± 0,7	25,5 ± 0,9
	60	17,7 ± 1,6	18,6 ± 0,9	20,6 ± 0,5	27,5 ± 0,8
	70	21,6 ± 3,3	19,6 ± 0,8	20,6 ± 0,3	25,5 ± 1,0
	100	23,5 ± 2,4	17,7 ± 0,7	21,6 ± 0,5	27,5 ± 1,7
6	0	24,5 ± 2,6	22,6 ± 0,5	28,4 ± 1,5	30,4 ± 1,8
	30	23,5 ± 2,0	20,6 ± 0,6	23,5 ± 0,5	29,4 ± 1,0
	40	22,6 ± 2,0	20,6 ± 0,7	26,5 ± 1,2	30,4 ± 0,6
	50	23,5 ± 2,8	22,6 ± 0,9	23,5 ± 1,3	30,4 ± 0,8
	60	23,5 ± 2,8	21,6 ± 0,8	22,6 ± 0,8	29,4 ± 1,1
	70	24,5 ± 2,4	19,6 ± 0,5	26,5 ± 1,3	31,4 ± 1,8
	100	25,5 ± 1,7	21,6 ± 0,8	23,5 ± 0,7	29,4 ± 1,9
6,5	0	27,5 ± 1,9	27,5 ± 1,3	28,4 ± 0,6	33,4 ± 2,1
	30	26,5 ± 2,6	26,5 ± 1,5	25,5 ± 0,5	33,4 ± 1,7
	40	26,5 ± 2,0	21,6 ± 0,7	26,5 ± 0,6	32,4 ± 0,5
	50	26,5 ± 3,4	27,5 ± 1,8	29,4 ± 0,8	32,4 ± 1,0
	60	24,5 ± 2,2	23,5 ± 0,9	30,4 ± 1,5	34,3 ± 0,8
	70	25,5 ± 2,8	27,5 ± 1,6	30,4 ± 1,1	33,4 ± 0,4
	100	27,5 ± 3,3	25,5 ± 1,0	26,5 ± 0,6	33,4 ± 2,1
7	0	30,4 ± 3,1	30,4 ± 2,0	33,4 ± 1,8	36,3 ± 1,1
	30	29,4 ± 2,3	24,5 ± 0,4	33,4 ± 1,3	36,3 ± 0,8
	40	27,5 ± 2,5	25,5 ± 0,4	33,4 ± 1,0	35,3 ± 0,8
	50	30,4 ± 3,2	26,5 ± 0,7	32,4 ± 1,4	35,3 ± 1,8
	60	29,4 ± 2,4	26,5 ± 0,7	29,4 ± 0,9	36,3 ± 2,1
	70	28,4 ± 1,7	28,4 ± 0,7	29,4 ± 0,5	35,3 ± 1,9
	100	31,4 ± 2,9	30,4 ± 1,3	32,4 ± 1,7	36,3 ± 1,3
7,5	0	32,4 ± 2,1	30,4 ± 2,0	37,3 ± 0,5	39,2 ± 1,4
	30	31,4 ± 2,9	32,4 ± 1,8	35,3 ± 1,5	38,3 ± 1,0
	40	30,4 ± 2,8	31,4 ± 1,6	35,3 ± 2,0	38,3 ± 1,6
	50	32,4 ± 3,1	33,4 ± 1,9	37,3 ± 1,1	37,3 ± 1,2
	60	32,4 ± 2,2	30,4 ± 1,3	36,3 ± 1,4	38,3 ± 1,2
	70	33,4 ± 2,2	34,3 ± 1,7	36,3 ± 1,0	38,3 ± 2,1
	100	34,3 ± 1,3	29,4 ± 1,1	36,3 ± 0,7	39,2 ± 1,4

Table 2. Measurement results for the load on the nozzle holder

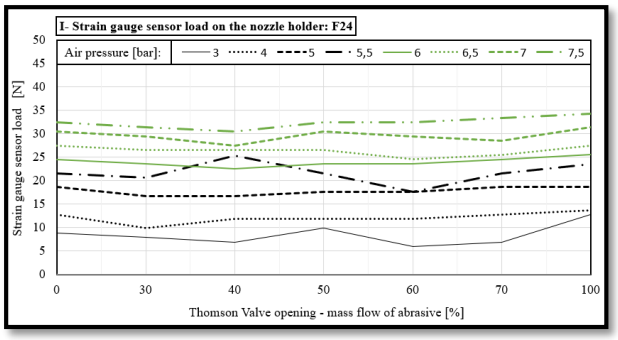


Figure 4. Load on the strain gauge sensor mounted on the nozzle holder-position I: Brown fused alumina F24

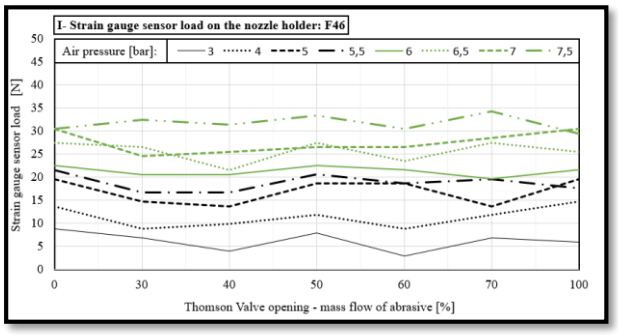


Figure 5. Load on the strain gauge sensor mounted on the nozzle holder-position I: Brown fused alumina F46

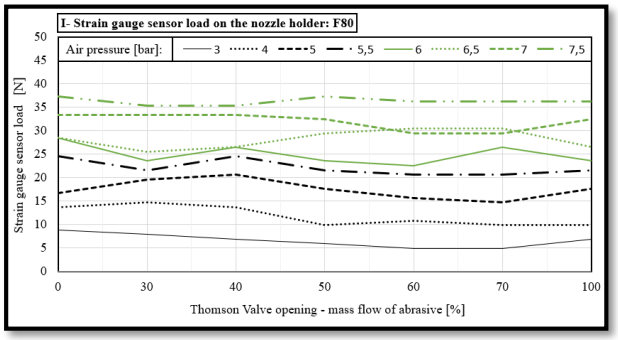


Figure 6. Load on the strain gauge sensor mounted on the nozzle holder-position I: Brown fused alumina F80

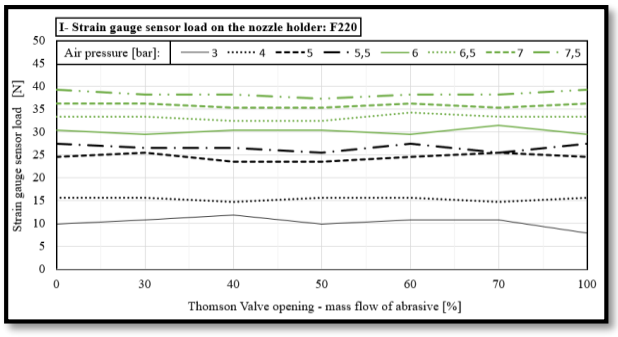


Figure 7. Load on the strain gauge sensor mounted on the nozzle holder-position I: Brown fused alumina F220

Air pressure [bar]	Mass flow [%]	Type of brown fused alumina			
		F24	F46	F80	F220
		Load on the blasting plate [N]			
3	0	12,2 ± 2,0	12,4 ± 1,2	13,1 ± 1,8	13,5 ± 1,7
	30	9,9 ± 1,8	10,0 ± 1,1	11,1 ± 1,7	12,7 ± 0,8
	40	9,1 ± 1,7	10,3 ± 0,6	11,1 ± 1,2	11,2 ± 2,3
	50	9,8 ± 3,5	11,7 ± 4,7	11,2 ± 1,8	12,9 ± 2,9
	60	9,4 ± 3,7	11,0 ± 2,6	9,8 ± 1,7	12,8 ± 1,6
	70	10,6 ± 3,1	11,6 ± 3,1	8,7 ± 2,9	13,2 ± 1,9
	100	10,5 ± 2,8	13,3 ± 2,9	13,2 ± 3,2	10,0 ± 3,3
4	0	17,1 ± 2,1	18,9 ± 1,9	17,3 ± 1,9	19,1 ± 2,1
	30	16,1 ± 1,7	16,9 ± 2,5	18,5 ± 1,5	19,5 ± 1,5
	40	15,0 ± 2,0	16,4 ± 1,8	17,6 ± 1,4	18,1 ± 2,2
	50	16,1 ± 5,2	16,8 ± 1,1	15,9 ± 2,8	18,8 ± 1,0
	60	17,4 ± 6,0	17,5 ± 1,3	15,9 ± 2,7	18,7 ± 2,1
	70	17,2 ± 5,3	17,0 ± 2,7	15,2 ± 2,8	19,7 ± 2,2
	100	18,4 ± 3,1	18,9 ± 4,3	16,6 ± 2,5	19,1 ± 1,3
5	0	23,6 ± 1,8	25,2 ± 1,2	25,6 ± 2,0	24,6 ± 2,3
	30	24,0 ± 1,5	22,9 ± 1,7	23,8 ± 3,0	25,0 ± 2,0
	40	22,2 ± 2,1	22,0 ± 1,3	23,6 ± 1,9	24,2 ± 0,9
	50	23,2 ± 3,7	24,0 ± 3,7	24,6 ± 1,4	23,3 ± 1,3
	60	22,8 ± 4,0	23,5 ± 4,2	24,5 ± 2,0	27,0 ± 2,1
	70	24,4 ± 5,3	22,7 ± 1,1	23,5 ± 3,5	23,2 ± 3,3
	100	23,2 ± 5,1	24,2 ± 4,5	23,7 ± 1,0	27,5 ± 3,4
5,5	0	28,2 ± 1,6	29,1 ± 1,4	28,9 ± 2,1	32,8 ± 0,9
	30	26,6 ± 1,8	25,8 ± 1,3	28,4 ± 2,1	29,0 ± 1,6
	40	25,3 ± 2,1	26,0 ± 1,3	27,9 ± 1,3	29,6 ± 1,4
	50	26,3 ± 5,2	26,5 ± 2,8	30,1 ± 5,2	26,3 ± 2,5
	60	23,6 ± 8,2	28,3 ± 4,7	28,4 ± 1,9	29,6 ± 3,3
	70	26,9 ± 6,0	26,2 ± 3,0	27,2 ± 1,1	30,7 ± 6,1
	100	28,7 ± 5,3	27,2 ± 5,2	27,9 ± 3,5	23,7 ± 7,7
6	0	32,1 ± 1,7	30,9 ± 1,2	32,1 ± 1,9	31,8 ± 2,2
	30	28,4 ± 1,6	30,5 ± 1,4	31,8 ± 1,7	32,7 ± 1,5
	40	29,3 ± 1,8	30,7 ± 1,7	33,1 ± 1,5	31,7 ± 1,4
	50	30,2 ± 5,2	30,9 ± 1,7	26,3 ± 1,5	31,8 ± 1,2
	60	30,4 ± 4,4	31,1 ± 5,1	29,8 ± 3,3	30,2 ± 3,2
	70	30,4 ± 4,7	29,9 ± 1,6	29,7 ± 4,2	32,2 ± 5,0
	100	33,2 ± 5,7	31,8 ± 3,9	25,6 ± 3,0	31,9 ± 3,1
6,5	0	35,9 ± 1,8	36,6 ± 2,3	37,2 ± 1,6	34,8 ± 3,0
	30	34,9 ± 1,4	33,7 ± 2,2	33,1 ± 2,1	35,5 ± 2,1
	40	32,7 ± 1,7	32,9 ± 2,1	35,1 ± 1,6	35,2 ± 2,1
	50	33,8 ± 3,2	34,4 ± 1,8	36,1 ± 1,6	34,7 ± 2,3
	60	32,3 ± 6,0	34,6 ± 2,4	33,5 ± 2,9	34,1 ± 2,2
	70	34,6 ± 4,2	35,8 ± 3,1	34,5 ± 2,6	35,9 ± 1,5
	100	33,8 ± 5,8	35,1 ± 3,0	34,2 ± 2,1	31,7 ± 3,5
7	0	37,6 ± 1,6	38,7 ± 1,6	35,5 ± 2,4	38,8 ± 1,5
	30	36,4 ± 1,8	36,1 ± 1,6	39,2 ± 0,9	39,9 ± 1,8
	40	37,6 ± 1,9	37,1 ± 2,1	37,1 ± 3,5	33,0 ± 1,8
	50	37,5 ± 2,9	37,5 ± 2,6	35,0 ± 4,5	39,6 ± 3,0
	60	38,5 ± 2,3	37,9 ± 1,3	38,2 ± 1,8	35,6 ± 4,9
	70	38,3 ± 5,7	37,0 ± 2,3	37,7 ± 2,2	34,1 ± 6,2
	100	39,2 ± 3,6	38,1 ± 2,3	36,8 ± 1,5	36,5 ± 2,2
7,5	0	40,2 ± 2,1	42,1 ± 2,9	31,3 ± 6,9	34,5 ± 2,5
	30	40,1 ± 1,6	40,6 ± 2,1	40,4 ± 2,1	39,4 ± 2,3
	40	38,2 ± 1,2	41,7 ± 3,1	37,4 ± 3,5	35,4 ± 2,8
	50	39,3 ± 2,0	40,5 ± 2,6	39,4 ± 3,8	32,5 ± 2,8
	60	41,5 ± 4,3	40,0 ± 1,8	38,9 ± 2,2	32,4 ± 2,4
	70	42,6 ± 4,1	39,8 ± 1,7	42,0 ± 1,9	31,4 ± 3,5
	100	42,6 ± 4,2	39,4 ± 2,2	35,3 ± 3,1	38,3 ± 2,7

Table 3. Measurement results for the load on the blasting plate

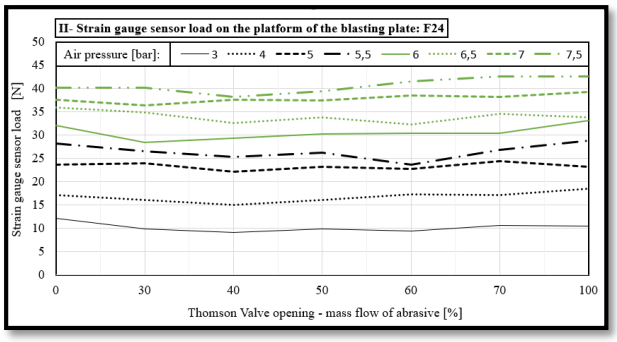


Figure 8. Load on the blasting plate platform measured by a strain gauge sensor-position II: Brown fused alumina F24

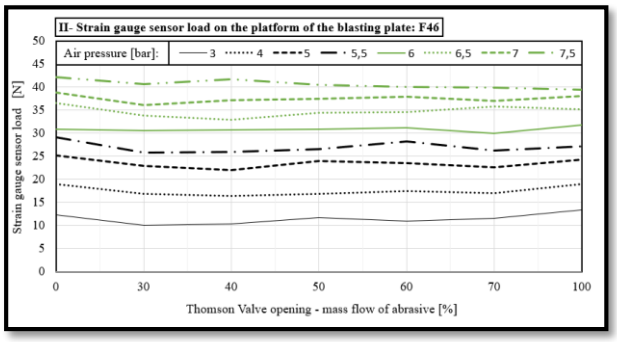


Figure 9. Load on the blasting plate platform measured by a strain gauge sensor-position II: Brown fused alumina F46

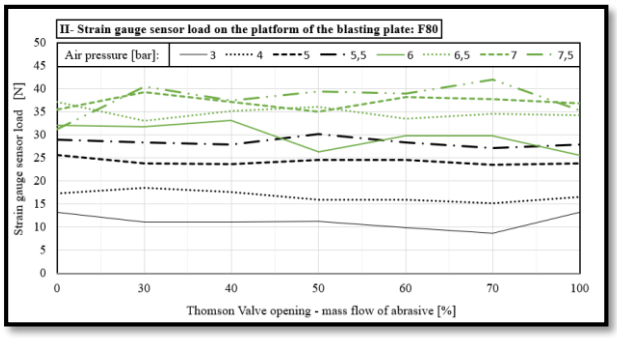


Figure 10. Load on the blasting plate platform measured by a strain gauge sensor-position II: Brown fused alumina F80

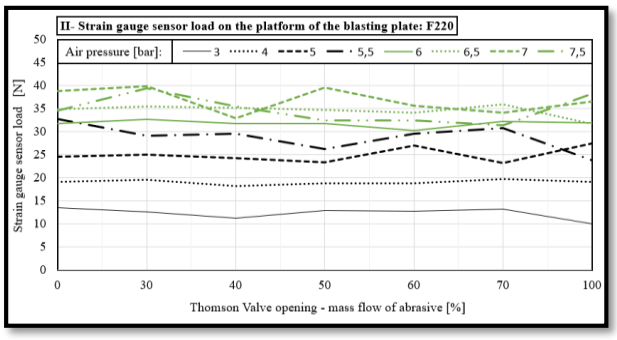


Figure 11. Load on the blasting plate platform measured by a strain gauge sensor-position II: Brown fused alumina F220

4 CONCLUSIONS

The results demonstrated the applicability of this method for automating adjustments to operating conditions in the blasting process and ensuring continuous operation. Experimental measurements showed that monitoring force using strain gauge sensor I on the nozzle holder and strain gauge sensor II on the blasting plate platform is effective for online monitoring of air pressure and is not sufficiently effective for online monitoring mass flow rate of abrasives during the blasting process. Based on the measured load on the nozzle and the blasting plate, the inlet air pressure can be clearly identified and monitored. For example, an inlet air pressure setting of 3 bar corresponds to a force of approximately 10 N, while a setting of 7.5 bar corresponds to a force of nearly 40 N. Strain gauge sensor I on the nozzle holder provides useful information about the magnitude of the force that the operator must maintain throughout the blasting cycle during manual blasting. Within the measured range, maximum force reached nearly 40 N, which represents increased physical strain on the operator that must be taken in to account in terms of job classification and occupational health and safety. Based on the experimental measurements performed, it can be concluded that measuring the force on the nozzle holder and on the blasting plate platform does not provide sufficiently comprehensive information for assessing the maximum efficiency of the blasting process. In the context of automating the blasting process, monitoring the forces at the nozzle outlet can serve as a control mechanism for the air pressure between the inlet and the outlet. In an industrial setting, the blasting process presents numerous risk factors that can lead to malfunctions, potentially disrupting operations or reducing blasting efficiency. Examples include the clogging of the hose line with an excess of abrasive material, or the kinking of a hose, both of which can significantly restrict the flow of air and abrasive.

ACKNOWLEDGMENTS

This article was created as part of Project No. CZ.02.01.01/00/22_008/0004631 “Materials and Technologies for Sustainable Development” under the Jan Amos Comenius Operational Program, funded by the European Union and the state budget of the Czech Republic, and the “European Fund for Just Transition” supported this work under the Just Transition Operational Program under the auspices of the Ministry of the Environment of the Czech Republic, CirkArena project, No. CZ. 10.03.01/00/22_003/0000045. The work was also supported by SGS grant no. SP2026/015, “Development of laboratory equipment for the comprehensive characterization of the rheological behaviour of heavy suspensions,” Faculty of Mining and Geology, VŠB – Technical University of Ostrava, Czech Republic.

REFERENCES

[Begg 2016] Begg, H., et al. Mechanization of the grit blasting process for thermal spray coating applications: a parameter study. Journal of Thermal Spray Technology, 2016, Vol. 25, pp. 12–20. DOI: 10.1007/s11666-015-0324-1.

[Bobzin 2016] Bobzin, K., et al. Influence of process parameter on grit blasting as a pretreatment process for thermal spraying. Journal of Thermal Spray Technology, 2016, Vol. 25, pp. 3–11. DOI: 10.1007/s11666-015-0297-0.

[CERABLAST 2026] CERABLAST. Minerals for blasting and flooring: Brown fused alumina, 2026. Available from: https://cerablast.com/en/brown-fused-alumina/.
[Glienke 2025] Glienke, R., et al. Effect of blast cleaning on the fatigue strength of welded and non-welded constructional details. Procedia Structural Integrity, 2025, Vol. 75, pp. 474-488. DOI: 10.1016/j.prostr.2025.11.048.
[Hansel 2000] Hansel, D. Abrasive blasting systems. Metal Finish, 2000, 98(6), 26–42. DOI: 10.1016/S0026-0576(00)80389-X.
[Int.EnviroGuard 2024] International Enviro Guard. Abrasive blasting: safety tips and PPE, 2024. Available from: https://int-enviroguard.com/blog/abrasive-blasting-safety-tips-and-ppe/.
[Kruszelnicka 2021] Kruszelnicka, W., et al. Study of the Relationships between Multi-Hole, Multi-Disc Mill Performance Parameters and Comminution Indicators. Sustainability, 2021, Vol. 13, No. 15, Art. no. 8260. DOI: 10.3390/su13158260.
[Mellali 1997] Mellali, M., et al. Alumina grit blasting parameters for surface preparation in the plasma spraying operation. Journal of Thermal Spray Technology, 1997, Vol. 6, pp. 217–227. DOI: 10.1007/s11666-997-0016-6.
[Momber 2016] Momber, A.W., et al. Statistical investigations into the flow of copper slag abrasive particles through a blast-cleaning metering system. Powder Technology, 2016, Vol. 301, pp. 179-185. DOI: 10.1016/j.powtec.2016.05.050.
[Nguyen 2024] Nguyen, V.B., et al. Optimal model-based control for automated robotized abrasive blasting system. Journal of Manufacturing Processes, 2024, Vol. 109, pp. 1-15. DOI: 10.1016/j.jmapro.2023.11.037.
[Pratap 2025] Pratap, A., et al. Ultrasonic assisted abrasive nano-blasting. CIRP Annals Manufacturing Technology, 2025, Vol. 74, pp. 459-463. DOI: 10.1016/j.cirp.2025.04.056.
[Varacalle 2006] Varacalle, D.J., et al. Effect of grit-blasting on substrate roughness and coating adhesion. Journal of Thermal Spray Technology, 2006, Vol. 15, pp. 348–55. DOI: 10.1361/105996306X124347.
[Zegzulka 2020] Zegzulka, J., et al. Characterization and flowability methods for metal powders. Scientific Reports, 2020, Vol. 10, Art. no. 21004.

CONTACTS:

Assoc. Prof. Eng. David Zurovec, PhD.

VSB-Technical University of Ostrava

Faculty of Mining and Geology

17. listopadu 15/2172, 708 00, Ostrava, Czech Republic

david.zurovec@vsb.cz

LICENSE CREATIVE COMMONS:

The article is published under the terms and conditions of the Creative Commons Attribution 4.0 International License (CC BY 4.0).